Kent Academic Repository

Kolipaka, Siva S., Junqueira, Laura A., Garg, Vivek, Trivedi, Vivek and Douroumis, Dennis (2026) ***Continuous manufacturing of 3D-printed chewable pediatric gummies by coupling hot melt extrusion with direct extrusion additive manufacturing.*** **Expert Opinion on Drug Delivery, 23 (6). pp. 1119-1131. ISSN 1742-5247.**

Downloaded from

https://kar.kent.ac.uk/113319/ The University of Kent's Academic Repository KAR

The version of record is available from

https://doi.org/10.1080/17425247.2026.2636173

This document version

Publisher pdf

DOI for this version

Licence for this version

CC BY-NC-ND (Attribution-NonCommercial-NoDerivatives)

Additional information

Versions of research works

Versions of Record

If this version is the version of record, it is the same as the published version available on the publisher's web site. Cite as the published version.

Author Accepted Manuscripts

If this document is identified as the Author Accepted Manuscript it is the version after peer review but before type setting, copy editing or publisher branding. Cite as Surname, Initial. (Year) 'Title of article'. To be published in ***Title of Journal*** , Volume and issue numbers [peer-reviewed accepted version]. Available at: DOI or URL (Accessed: date).

Enquiries

If you have questions about this document contact ResearchSupport@kent.ac.uk. Please include the URL of the record in KAR. If you believe that your, or a third party's rights have been compromised through this document please see our Take Down policy (available from https://www.kent.ac.uk/guides/kar-the-kent-academic-repository#policies).

Expert Opinion on Drug Delivery

ISSN: 1742-5247 (Print) 1744-7593 (Online) Journal homepage: www.tandfonline.com/journals/iedd20

Continuous manufacturing of 3D-printed chewable pediatric gummies by coupling hot melt extrusion with direct extrusion additive manufacturing

Siva S. Kolipaka, Laura A. Junqueira, Vivek Garg, Vivek Trivedi & Dennis Douroumis

To cite this article: Siva S. Kolipaka, Laura A. Junqueira, Vivek Garg, Vivek Trivedi & Dennis Douroumis (2026) Continuous manufacturing of 3D-printed chewable pediatric gummies by coupling hot melt extrusion with direct extrusion additive manufacturing, Expert Opinion on Drug Delivery, 23:6, 1119-1131, DOI: 10.1080/17425247.2026.2636173

To link to this article: https://doi.org/10.1080/17425247.2026.2636173

© 2026 The Author(s). Published by Informa UK Limited, trading as Taylor & Francis Group.

View supplementary material

Published online: 28 Feb 2026.

Submit your article to this journal

Article views: 976

View related articles

View Crossmark data

Citing articles: 3 View citing articles

Full Terms & Conditions of access and use can be found at
https://www.tandfonline.com/action/journalInformation?journalCode=iedd20

EXPERT OPINION ON DRUG DELIVERY
2026, VOL. 23, NO. 6, 1119–1131
https://doi.org/10.1080/17425247.2026.2636173

Taylor & Francis
Taylor & Francis Group

ORIGINAL RESEARCH

OPEN ACCESS Check for updates

Continuous manufacturing of 3D-printed chewable pediatric gummies by coupling hot melt extrusion with direct extrusion additive manufacturing

Siva S. Kolipaka[a], Laura A. Junqueira[b], Vivek Garg[c], Vivek Trivedi[d] and Dennis Douroumis[b,e]

[a]Centre for Research Innovation (CRI), University of Greenwich, Chatham, UK; [b]Research and Development Department, Delta Pharmaceutics, Chatham, UK; [c]Wolfson Centre for Bulk Solids Handling Technology, Faculty of Engineering & Science, University of Greenwich, Chatham, UK; [d]Medway School of Pharmacy, University of Kent, Chatham Maritime, UK; [e]School of Life and Health Sciences, Department of Health Sciences, University of Nicosia, Athens, Greece

ABSTRACT

Background: 3D printing has been extensively explored as a novel approach to fabricating customized pharmaceuticals due to its adaptability. In this study, a continuous 3D (3-dimensional) printing platform was developed for the fabrication of chewable, gummy-like pediatric tablets by coupling Hot Melt Extrusion and Direct Extrusion Printing.

Research design and methods: The effects of polymer composition, super disintegrants, and infill density on extrusion, printability, and structural integrity were systematically evaluated. Rheological analysis revealed that optimized inks exhibited stable shear-thinning behavior as low as 1.0×10^5 to 1.0×10^6 mPa/s with increasing shear rates, ensuring smooth extrusion and excellent layer adhesion. *In vitro* dissolution studies demonstrated that tablet geometry, infill density, and ink composition could be tailored to achieve immediate drug release.

Results: 30% and 50% infill structures provided reduced compressive resistance suitable for soft, chewable tablets and resulted in nearly 90% drug release within 30 min. Sensory assessment confirmed effective taste masking via hydrogen-bonding interactions, and optimized sweetener – flavor ratios ensured palatability.

Conclusions: 3D printing enabled the production of pediatric-friendly, chewable dosage forms with tailored mechanical, dissolution, and sensory properties, supporting personalized medicine and enhanced patient compliance.

ARTICLE HISTORY
Received 16 December 2025
Accepted 12 February 2026

KEYWORDS
Direct 3D printing; continuous manufacturing; chewable tablets; pediatric; hot melt extrusion; taste masking

1. Introduction

Chewable tablets (CTs) are "oral solid dosage forms designed to be chewed and subsequently swallowed by the patient instead of being ingested whole [1]. CTs gained great attention due to their ease of administration, suitable for pediatrics, geriatrics, and dysphagic populations who may have difficulty swallowing [2]. Their ease of administration, rapid onset of action, and the fact that they do not require water make them an attractive alternative to traditional oral tablets and capsules. From the formulation perspective, the development of chewable tablets involves unique challenges and considerations, such as taste masking of bitter APIs [3] optimizing mouthfeel and ensuring adequate mechanical strength without compromising chewability [4,5]. In the wake of pharmaceutical processing technologies such as hot melt extrusion, direct extrusion printing (3D) [6], chewable tablets have evolved into more sophisticated delivery systems capable of incorporating immediate and modified-release profiles, high drug loads, and a combination of drugs [7,8].

Hot-melt extrusion (HME) is a powerful, versatile, and efficient technology that has gained widespread application in pharmaceutical manufacturing, providing innovative solutions for drug formulation and delivery [9–11]. It is particularly effective in enhancing the solubility and bioavailability of poorly water-soluble drugs, especially those categorized under the Biopharmaceutics Classification System (BCS) Classes II and IV [12,13]. During the extrusion process, the melting and intimate mixing of active pharmaceutical ingredients (APIs) within a polymeric matrix result in the formation of amorphous solid dispersions (ASDs) [14,15]; which enhance drug solubility by improving wettability and reducing crystallinity. Moreover, the solvent-free nature of HME aligns with current environmental and regulatory requirements, promoting greener pharmaceutical manufacturing practices [10,16]. Another key advantage of HME is its compatibility with continuous manufacturing approaches [17], supporting the industry's transition toward more efficient, scalable, and cost-effective production systems. The homogeneous extrudates obtained from HME can be further processed into diverse solid dosage forms, including tablets, films, pellets, and filaments for 3D printing [18]. However, HME requires elevated processing temperatures, which can lead to thermal degradation of heat-sensitive active pharmaceutical ingredients and

CONTACT Siva S. Kolipaka S.Kolipaka@gre.ac.uk Centre for Research Innovation (CRI), University of Greenwich, Chatham ME4 4TB, UK; Dennis Douroumis Douroumis.d@unic.ac.cy School of Life and Health Sciences, Department of Health Sciences, University of Nicosia, 29th Street, No. 17, Elliniko, Athens 167 77, Greece

Supplemental data for this article can be accessed online at https://doi.org/10.1080/17425247.2026.2636173

© 2026 The Author(s). Published by Informa UK Limited, trading as Taylor & Francis Group.
This is an Open Access article distributed under the terms of the Creative Commons Attribution-NonCommercial-NoDerivatives License (http://creativecommons.org/licenses/by-nc-nd/4.0/), which permits non-commercial re-use, distribution, and reproduction in any medium, provided the original work is properly cited, and is not altered, transformed, or built upon in any way. The terms on which this article has been published allow the posting of the Accepted Manuscript in a repository by the author(s) or with their consent.

Table 1. Ink composition of IBU chewable tablets.

Inks		F1	F2	F3	F4	F5	F6	F7	F8	F9
S. no.	Ingredients					%w/w				
1	Ibuprofen	40.0	40.0	40.0	35.0	35.0	35.0	30.0	30.0	30.0
2	EPO	15.0	10.0	10.0	10.0	10.0	10.0	10.0	10.0	10.0
3	EPO Ready Mix	–	5.0	5.0	5.0	5.0	5.0	5.0	5.0	5.0
4	US2	–	–	–	6.0	10.0	10.0	15.0	15.0	15.0
5	GalenIQ	30	30	20.0	–	20	25	25	25	25
6	Xanthan	10.0	10.0	10.0	19.5	5.0	4.0	4.0	–	–
7	PVP-XL	–	–	–	–	–	–	5.0	5.0	–
8	CCS	–	–	–	–	–	–	–	4.0	9.0
9	Starch			10.0	19.5	10.0	5.0	–	–	–
10	Sucralose	2.0	2.0	2.0	2.0	2.0	2.0	2.0	2.0	2.0
11	Orange	3.0	3.0	3.0	3.0	3.0	3.0	3.0	3.0	3.0
Total (%w/w)		100.0	100	100.0	100.0	100.0	100.0	100.0	100.0	100.0

excipients. Prolonged exposure to high temperatures may also promote chemical instability or recrystallization of amorphous drugs. Consequently, the applicability of HME is limited for thermolabile compounds without the use of plasticizers or alternative low-temperature processing strategies [19]. Recently, pharmaceutical 3D printing [20,21] has been explored as a novel approach for the fabrication of customized pharmaceuticals by adaptability in dosage, shape, and design, perhaps with the potential to improve acceptance among the pediatric population [22,23]. Among the various 3D printing techniques, direct extrusion 3D printing has gained increasing attention for its suitability in processing pharmaceutical materials under mild conditions [24]. Unlike fused deposition modeling (FDM), which requires thermoplastic filaments, direct extrusion operates by extruding pellets or powders directly through a nozzle, avoiding the limitations of filament-based systems [25]. This framework presents an innovative approach for the continuous manufacturing of chewable tablets using ASDs produced via HME, which are pelletized and introduced directly into the printhead for printing by direct extrusion of the final dosage forms, circumventing the printability challenges of filaments [26,27]. As the pharmaceutical industry increasingly shifts toward patient-centric and decentralized manufacturing, direct extrusion 3D printing enables the production of complex geometries, supporting the development of personalized medicines and stands out for its potential in drug fabrication, especially in clinical studies, pharmacies, and remote areas [28–30] Specifically, the coupling of HME with direct extrusion 3D printing enables a compact, continuous, and modular manufacturing workflow suitable for point-of-care settings. This integrated approach allows on-demand production of personalized dosage forms without the need for intermediate filament preparation or large-scale infrastructure. As a result, it supports decentralized manufacturing by offering flexibility, rapid turnaround, and reduced supply chain dependence [31].

Here, we introduce a continuous 3D printing platform by coupling HME and direct extrusion printing for the design and fabrication of personalized pediatric dosage forms. The inks were designed to improve the palatability, printability, and structural integrity of printed structures with consistent printing quality throughout the manufacturing process.

2. Material and methods

2.1. Materials

Ibuprofen (IBU) was obtained from Farmasino Pharmaceuticals Co., Ltd. (Nanjing, China). Eudragit EPO and EPO Ready Mix were sourced from Evonik (Darmstadt, Germany). Neusilin US2 (NEU) was supplied by Fuji Chemical Industries Co., Ltd. (Japan), GalenIQ 981 (Isomalt) was acquired from BENEO GmbH (Mannheim, Germany), Starch 1500 was purchased from Colorcon (Indianapolis, IN, U.S.A.), Polyplasdone XL (Crospovidone) and croscarmellose sodium (CCS) were obtained from JRS Pharma (Cedar Rapids, U.S.A.). Xanthan gum was sourced from Jordanian Pharmaceutical Company Ltd., Sucralose was purchased from Merck (Germany), and orange flavor from TasteTech (Southeast Bristol, UK).

2.2. Ink design and blend preparation

As shown in Table 1, a range of compositions (inks) was designed for the manufacturing of 3D printed gummy-like chewable designs. For each ink, the bulk powders were firstly sieved through a 500 µm mesh and subsequently blended using a Turbula shaker-mixer (Glen Mills T2F Shaker/Mixer, U.S.A.) at 34 rpm for 10 minutes to ensure homogeneity.

2.3. Hot melt extrusion

The resulting physical blends were processed using a 10 mm Rondol Micro lab twin screw extruder (Rondol, France) with a 25:1 length-to-diameter ratio. The standard screw conFigureuration comprised two kneading zones: the first zone had 30° and 45° discs (six of each), while the second zone had 30° (three discs) and 90° (nine discs). The barrel temperatures for the five heating zones were set to 80°C, 90°C, 90°C, 90°C, and 85°C (from feed to die), and the screw speed was set at 100 rpm. Each batch size was 50 g, fed at a rate of 150 g/h. The extruded strands were pelletized into 2 mm pellets using a Rondol strand pelletizer (Nancy, France).

2.4. Rheology

Anton Parr MCR 302 Rheometer (Anton Parr GmbH in Graz, Austria) was used to examine the rheological properties of extruded filaments F2, F4, F7, and F9 under the conditions 10°C above the extrusion temperature. A series ($n = 3$) of experiments was performed to ascertain the viscosity of F2, F4, F7, and F9 at temperatures of 70°C, 70°C, 80°C, and 85°C, respectively. The melt viscosity of the inks was assessed using a flat 25PP upper geometry with a 1 mm gap. The shear rates used for the measurement varied from 0.01 to 10 s^{-1} (1 s^{-1}) versus viscosity between 1×10^{04} to 1×10^{09} [26].

2.5. Design and 3D printing of chewable gummy-like IBU designs

The chewable gummy-like structures were designed using SolidWorks software (Dassault Systems, U.S.A.) in the shapes of a heart and a disk. The design was converted into a.stl file and sliced by Simplify 3D software (Simplify 3D LLC, U.S.A.), which generates the printing path for the 3D printer. The chewable tablets were printed by a Tumaker NX Pro Pellets (Tumaker, Spain) printer using the IBU-loaded pellets previously prepared.

The 3D printing parameters were conFigureured as follows: the output temperature (nozzle) was set at 90°C, the inlet temperature (screw) was maintained at 80°C, and the build plate temperature was kept at 25°C. Printing speed was optimized at 4000 mm per minute, with a layer height of 0.4 mm. The extrusion multiplier of 1.5% was applied to ensure accurate and consistent material deposition during the printing process. Tablets were printed with varying infill densities of 100%, 70%, 50%, and 30%.

2.6. Mass uniformity (drug content, dose accuracy, and content uniformity) and dimensional accuracy

An analytical balance (Mettler Toledo; XS105 dual-range balance) was used to weigh each printed unit, and mean weight, standard deviation (SD), and acceptance limits were calculated according to pharmacopoeial guidelines. A digital Vernier calliper (Mahr U.K. Ltd.) was used to measure the length, width, and thickness of each structure to check for dimensional correctness ($n = 5$). The IBU content of printed structures was quantified using the analytical protocol detailed in section 2.13. Each sample was dissolved in 25 mL of ethanol under stirring at 250 rpm for 60 minutes, diluted as required, and analyzed via HPLC. The measured dose and dose accuracy (±15% acceptance criteria) were calculated relative to the theoretical 100 mg IBU/tablet. Content uniformity was assessed according to pharmacopoeial standards (USP – NF 2024, 1 May 2024), requiring individual units to fall within 85–115% of the label claim.

2.7. Thermogravimetric analysis (TGA)

TGA analysis of the bulk IBU and excipients was conducted using a TGA 5500 instrument from TA Instruments (Crawley, UK). About 3 to 5 mg of each sample was placed in Tzero aluminum crucibles. The crucibles were then positioned in the TGA sample holder and heated from 25°C to 250°C at a rate of 10°C per minute, and a constant nitrogen flow of 25 mL/min was maintained throughout the experiment.

2.8. Differential scanning calorimetry (DSC) analysis

DSC (DSC823e, Mettler-Toledo, LLC, Leicester, UK) was used to examine the bulk IBU, excipients, and inks. A nitrogen flow of 50 mL/min was consistently maintained throughout the analysis. All the samples were weighed between 4 to 8 mg and were placed in the aluminum crucibles and sealed with lids. The sealed pans were thereafter positioned in the DSC sample holder and heated at a rate of 10°C/min. The thermogram was recorded at temperatures ranging from 50 to 160°C.

2.9. X-ray powder diffraction (XRPD)

X-ray powder diffraction (XRD) was performed on individual materials and processed inks using a Bruker D8 Advance diffractometer (Bruker, Karlsruhe, Germany) in theta-theta reflection mode with a copper anode. The samples were scanned from 0° to 60° with a 0.6-millimeter slit and a step size of 0.02°. Data analysis was carried out using EVA software (version 5.2.0.3, Bruker AXS, Germany).

2.10. Scanning electron microscopy (SEM)

Scanning electron microscopy (SEM) was employed to examine the surface morphology of the bulk IBU and the 3D-printed chewable tablets. The samples were affixed to an aluminum stub utilizing conductive carbon adhesive tape (Agar Scientific, Stansted, UK), followed by the coating with approximately a 10-nanometer gold layer. Micrographs were obtained with a Hitachi SU8030 scanning electron microscope (Hitachi High-Technologies, Maidenhead, UK) with an accelerating voltage of 10kV and magnifications of 30X.

2.11. Attenuated total reflectance-fourier transform infrared (ATR-FTIR) spectroscopy

A Range Two FTIR spectrometers (Perkin Elmer, UK) were utilized to record the ATR-FTIR spectrum of the drug, polymers, and inks. A zinc selenide (ZnSe) crystal-equipped solitary reflection, horizontal ATR accessory was utilized to ensure uniform distribution of the sample across its surface. Spectra were obtained in the range of 4000 to 400 cm^{-1} using percentage (%) transmission mode.

2.12. Texture profile analysis

The texture analysis was performed using a TA.XTplusC Texture Analyzer (Stable Micro Systems, Godalming, United Kingdom) equipped with a 10-kg load cell. A cylindrical aluminum probe (35 mm diameter) was applied in a compression test at a speed of 1 mm/s [24]. IBU 3D printed chewable tablets were evaluated, with five samples tested for each ink. The dimensions of the tablets were determined as per the method described in section 2.6. The whole tablet was used

for texture analysis, and all samples were tested using identical tablet geometries to ensure comparability across formulations. Texture analysis was performed using a double-compression test, with deformation defined by probe displacement rather than percentage strain. The standard parameters measured included hardness, cohesiveness, springiness, gumminess, and chewiness.

The height of the initial force peak serves as an indicator of hardness, and the ratio of the area of the first peak (area between anchors 1 and 3) to that of the second peak (anchors between 4 and 6) serves as an indicator of cohesiveness. Springiness refers to the temporal measurement of the detected height during the second compression in relation to the corresponding value during the first compression. Chewiness results from the product of chewiness and springiness. Gumminess results from the product of Hardness and Cohesiveness. The negative space between two compressions is referred to as adhesion. The peaks are illustrated in Figure S1 (supplementary), showing anchors numbered 1 to 6, respectively.

Anchor 1 = Starting point of the experiment.
Anchor 2 = Point of highest force for the first peak.
Anchor 3 = End of first peak (when it goes back to zero).
Anchor 4 = Where the second peak starts.
Anchor 5 = Point of highest force in the second peak.
Anchor 6 = Where the second peak goes back to zero.

2.13. In-vitro *dissolution studies and HPLC analysis*

The bulk IBU, IBU-loaded pellets, and 3D printed tablets equivalent to 100 mg of IBU ($n = 3$), were analyzed using the USP Type II paddle method [32]. The pH of the dissolution media was initially pH 1.2 ± 0.05 for fifteen minutes; thereafter, a few drops of 10% sodium hydroxide were added to elevate the pH to 7.2 ± 0.05. The FDA suggests evaluation across pH 1.2, 4.5, 6.8, and water to characterize chewable tablets, but it does not require all media to be tested separately in every study. For IBU chewable tablets, pH 7.2 is clinically relevant and an FDA-accepted dissolution medium [33]. The applied pH-shift method captured both the initial acidic exposure in the gastric environment and the subsequent drug release at higher pH in a single experiment, providing an assessment of dissolution behavior relevant to the intended site of drug release. The temperature was maintained at 37 ± 0.5°C, and the paddle speed was set at 50 rpm while the samples were carefully introduced into 900 mL of dissolving medium. 5 mL of the aliquot sample was collected from the dissolution bowl at time intervals of 5, 10, 15, 30, 45, and 60 minutes. Thereafter, fresh medium of equal volume was added. The collected samples were filtered using 0.45 µm PES syringe filters (Merck, Germany) and quantified using HPLC [34].

All dissolution samples were examined using a high-performance liquid chromatography system (Agilent Technologies, 1200 series, U.S.A.) to quantify the concentrations of IBU. The configuration included a UV detector and a C18 HICHROM S5ODS1-11221 column, measuring 250 mm in length, 4.6 mm in diameter, and possessing a porosity of 250 Å, with a particle size of 5 µm. The mobile phase was composed of a 1:1 ratio of 0.2% phosphoric acid buffer and acetonitrile. The detecting wavelength was established at 214 nm, and the mobile phase flow rate was 1.5 mL per minute with ambient column temperature.

2.14. *Sensory evaluation of taste masking*

The taste-masking experiment on the bulk IBU, EPO, EPO ready mix, xanthan gum, starch, a 3D printed heart, and a 3D printed tablet (cylinder) was conducted after obtaining informed consent from 10 healthy human subjects, approved by the University of Greenwich's Ethics Committee (protocol code reference number: UG09/10.5.5.12 May 2021). The participants, aged 18 to 30, included both men and women. Each was instructed to place a small amount of the sample in their mouth, taste it for 30 to 60 seconds, and then spit it out. They were also told to rinse their mouths thoroughly with fresh water after each sample. During the study, participants were clearly instructed not to ingest the samples. A 5-point scale was used to rate the bitterness of the bulk materials and 3D printed products, where scores of 1, 2, 3, 4, and 5 indicated extremely bitter, considerably bitter, mildly bitter, slightly bitter, and no bitter taste, respectively. For sweetness evaluation, a panel of 10 participants assessed GalenIQ, sucralose, and 3D-printed tablets, and their responses were recorded using the following categories: no sweetness, moderate sweetness, very sweet, extremely sweet, and aftertaste. Similarly, orange aroma perception was evaluated for the orange flavoring and 3D printed tablet, and panelists rated the samples using the descriptors sweet, orange, sour, fruity, and aftertaste. This method was adapted from the work of [26]

2.15. *Statistical analysis*

Statistical analysis was performed for *in-vitro* dissolution performances of 100% and 30% infill densities of 3D printed chewable tablets using the Two-way ANOVA, and statistical significance was set at $p < 0.05$ using Fusion One software (DoE Fusion One TM, California, United States).

3. Results and discussion

3.1. *Ink design and material selection*

The primary objective of this study was to establish a continuous manufacturing platform for the 3D printing of chewable, gummy-like pediatric dosage forms. Aprecia, Triastek, and FabRx have developed GMP-compliant 3D printers for pharmaceutical use. Triastek and FabRx further advanced extrusion-based 3D printing by employing powdered materials, eliminating the need for filament preparation. Here, we introduce a platform where HME is coupled with direct extrusion printing of the produced drug-loaded pellets. The extruded inks are fed to the conveyor and the pelletizer, where rods with sizes varying from 1–3 mm are produced (Figure S2, supplementary). Subsequently, the pellets are fed directly to a dual printer, and the printing of the dosage forms is carried out in a continuous mode.

As summarized in Table 1, the IBU-loaded ink was systematically designed through the careful selection of suitable

excipients. Based on preliminary investigations, EPO and EPO-ready mix were employed to enhance the solubility of IBU, while NEU was incorporated to mitigate excessive polymer plasticization associated with high drug loading. Xanthan gum, CCS, Polyplasdone XL, and Starch 1500 were chosen for their proven ability to form flexible, chewable matrices, and enhance the disintegration and potentially enhance the dissolution rates. The influence of each polymer on the printability of the inks was further assessed by varying their ratios to optimize both mechanical and processing performance.

GalenIQ 981 was incorporated as a taste masking agent, but also as a filler to aid the printability of the designed inks. Finally, sucralose and orange flavor were added to improve the palatability of the printed dosage forms.

3.2. Thermal and X-ray analysis

Prior to extrusion optimization, thermal analysis for the bulk materials was carried out by using TGA and DSC. In Figure 1, the TGA thermograms revealed that all materials were thermally stable at high temperatures, while IBU (started to be degraded at 130 °C) and sucralose up to 140°C. In addition, some water loss was observed for GalenIQ and the orange flavor.

The DSC thermogram of the bulk IBU showed sharp endothermic peaks at 79.31°C (Figure 2), due to its unique crystalline structure. As shown in Figure S3 (supplementary), the EPO and GalenIQ presented glass transition temperatures at 52°C and 101.09°C, respectively.

Based on the TGA analysis, it was concluded that HME processing temperatures shouldn't exceed 90–100°C. Thermal analysis was also conducted for the extruded inks (in the form of pellets) and the printed structures. In Figure 2, the thermograms show the absence of IBU melting endotherms due to the drug transformation into an amorphous state or solubilization in the melted excipients during the heating cycle.

To confirm the DSC findings further, X-ray analysis was conducted for the bulk materials (Figure S4, supplementary), the extrudates, and the 3D printed chewable tablets. Figure 3 shows the lack of IBU intensity peaks across the obtained diffractograms for both the extruded and printed samples. The presence of small intensity peaks at various 2θ values was associated with those of EPO Ready Mix and GalenIQ. Hence, the X-ray analysis confirmed the complete IBU transformation into an amorphous state in the course of HME processing.

3.3. Extrusion and printability optimization

During the HME processing, it was found that the EPO/EPO ready mix/NEU ratios were critical for the extrusion optimization, as they significantly affected the printability of the inks.

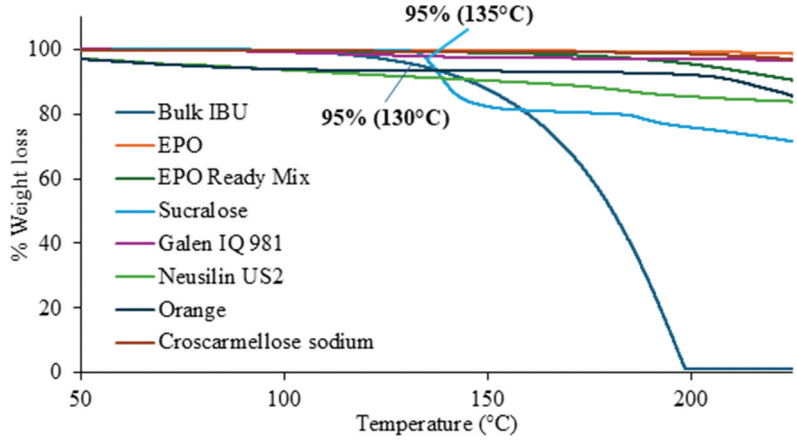

Figure 1. TG Thermograms of the bulk materials used for the printing inks.

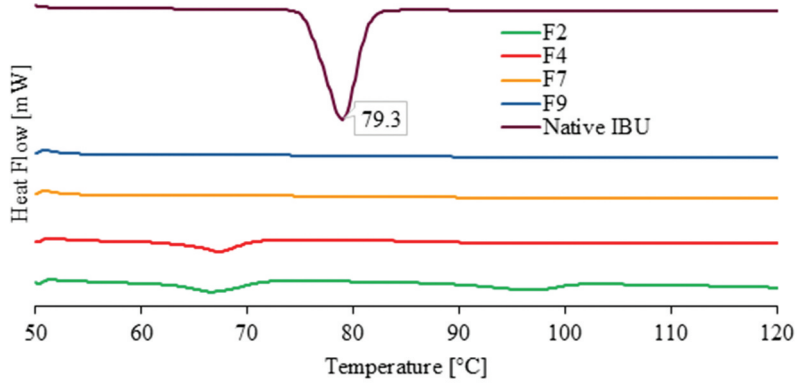

Figure 2. DSC thermograms of the bulk IBU, extruded inks, and 3D printed chewable tablet.

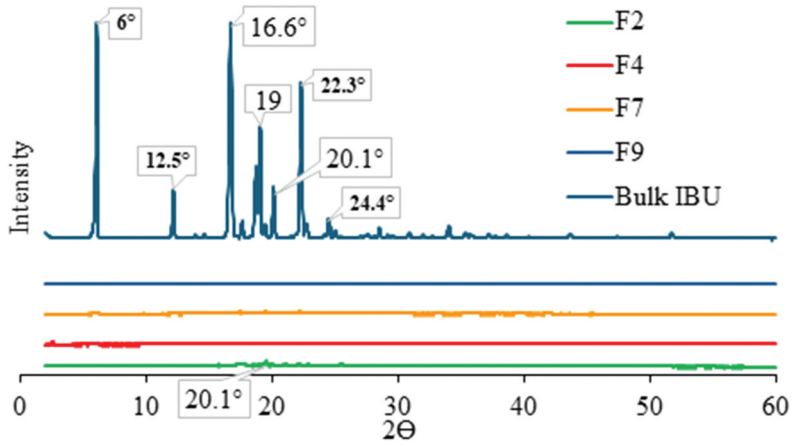

Figure 3. X-ray diffractograms of the bulk IBU, extruded inks, and 3D printed chewable tablet.

Similarly, the presence of xanthan gum, starch, GalenIQ, and CCS showed a pronounced effect on the quality of the extruded pellets and printed structures at the final step.

As illustrated in Table 1, the F2 and F4 inks were printable, although flow issues were observed, but they failed to maintain their shape after printing (Supplementary Figure S5). High amounts of xanthan gum and starch had a negative effect on the printability and shape stability of the structures due to their strong plasticization effect with IBU. Hence, their percentage was further reduced while the NEU (magnesium aluminometasilicate) was increased to reduce plasticization and tackiness of the prints. Further optimization showed that the addition of low superdisintegrant amounts improved printability.

As a result, the F7 and F9 maintained their structure and shape after printing, where the latter demonstrated superior printability in comparison to the other compositions. The above findings could be justified by analyzing the rheological properties of the extruded compositions. The melt viscosities of pharmaceutical compositions for the manufacturing of gummy-like dosage forms always pose challenges in 3D printing, due to their thinning behavior. Figure 4 illustrates the viscosity of selected compositions with shear rates varying from 0.01 to 10.0 sec. As can be seen, all extruded inks presented non-Newtonian shear thinning behavior, which was profoundly affected by the used composition. From Figure 4, it is obvious that most inks demonstrated strong shear thinning performance with shear viscosities as low as $1.0x10^{05}$ to $1.0x10^{06}$ mPa/s with increasing shear rates. This was attributed to the excessive plasticization effect of IBU in the presence of Polyplasdone-XL, xanthan gum, and starch, and the high drug loading.

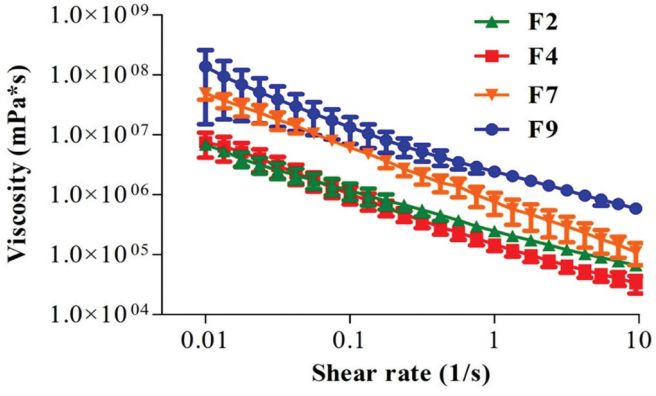

Figure 4. Rheological evaluation of extruded compositions at 100°C (print temperature).

To the contrary, the viscosity of F9 exhibited only a tenfold change and decreased from $1.0x10^{08}$ to $1.0x10^{07}$ mPa/s. As a result, for printing temperatures as high as 100°C, the desired extrudability and perfect layer adhesion were achieved. By reaching a stable viscosity profile for F9, a consistent flow through the nozzle was attained, which resulted in smooth printing and excellent shape retention. It was observed that the presence of CCS reduces the plasticization effect and maintains viscosity at the required standards. For most of the inks, the printability was modest, but the printed designs couldn't self-support and structures collapsed over a period (24 h) at ambient temperatures.

For the development of printed gummy-like chewable tablets, the printing settings were optimized to ensure adequate material extrusion. The tablet size and shape were designed to achieve a dosage of 100 mg of IBU with a total object weight of 334 mg (aspect ratio 1:1). Rutuja Mundhe et al. [35] reported that prolonged mastication of chewable tablets can lead to facial muscle discomfort. To mitigate this potential issue, chewable tablets with varying infill densities were fabricated in the present study. This level of structural control is solely feasible through 3D printing, which allows the production of structures with customizable internal architecture such as honeycomb, rectilinear, circular, or triangular infill patterns, while preserving overall mechanical integrity.

As shown in Figure 5, the optimization resulted in excellent printability, producing a 3D structure identical to the design file without any printing failures. The total printing time for each structure was 70–75 s when using a 0.4 mm printing nozzle. To reduce the print time for each design the nozzles size the effect of the nozzle size was investigated. By using printing nozzles of 0.6 mm diameter, the print time was reduced to 55–60 s per object, while for a 0.8 mm nozzle

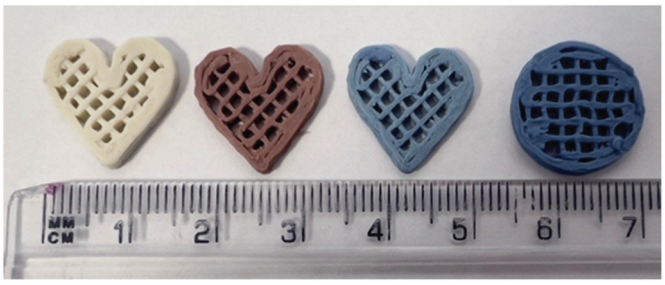

Figure 5. Direct extrusion 3D printed gummy-like chewable designs loaded with IBU (F9) at aspect ratio 1:1 and nozzle size 0.4 mm.

diameter, to 45-50s, without compromising the product quality of printing.

3.4. Dimensional accuracy of 3D printed gummy-like structures

The dimensional accuracy of the 3D-printed gummy-like structures was highly reproducible for both inks (F7 and F9) across all infill densities (Table 2). Measurements of length, width, thickness, and printed dose weight showed very low standard deviations, indicating excellent printability and dimensional stability.

3.5. Mass and content uniformity of 3D printed gummy-like structures

The individual weights of each 3D-printed gummy-like dosage form were used to determine the upper and lower mass limits for the two ink compositions selected for further evaluation. As shown in Table 3, all samples fell within the specified limits and met the acceptance criteria, with no individual weight deviating from the mean mass by more than 5%. Similarly, drug content and dose accuracy were evaluated for the two IBU ink compositions. The dose accuracy results were satisfactory, with all values exceeding 90%. Furthermore, the content uniformity of both batches complied with pharmacopoeial standards, with measured IBU content ranging between 95% and 105% of the label claim. Consistent mass uniformity was achieved across all gummy-like structures, irrespective of the ink composition, as illustrated in Table 3.

Measured dose, dose accuracy, and content uniformity were assessed as critical quality attributes of the 3D-printed gummy-like dosage forms. All units complied with mass uniformity requirements, showing deviations within ±5% of the mean. Measured IBU doses closely matched the theoretical value and remained within the acceptable ±15% accuracy range. Individual content uniformity results confirmed homogeneous drug distribution, with contents between 95% and 105% of the label claim. Measured content uniformity (%) expresses the drug content of each printed unit as a percentage of the theoretical label claim. Collectively, these results demonstrate precise dose control and robust reproducibility regardless of ink composition.

3.6. Micrographs of 3D printed tablets

As shown in Figure 6(a), the surface morphology of 3D-printed objects presented a smooth surface finish without any defects, indicating excellent print quality and ease of the printing process. The absence of any IBU crystals on the surface was indirect proof that the drug was fully embedded in the polymer matrix. By observing Figure 6(b), it is evident that layer thickness was highly consistent and around 0.30–0.32 mm despite the rapid print speeds [36]. The apparent difference between the set layer thickness (0.4 mm) and the measured layer thickness (300–316 µm) was due to the controlled compression of the extruded filament during printing. Upon deposition, the extrudate slightly flattens to create a uniform surface that enhances interlayer adhesion and structural stability. This behavior has been reported previously and is typical in direct extrusion printing and was intentionally employed to achieve consistent layer bonding and optimized print quality [37,38]. This suggests excellent printability with a consistent flow of the print ink during the direct extrusion printing processing, which resulted in great layer adhesion.

3.7. FTIR analysis

As shown in Figure 7, the FTIR spectra of the bulk IBU and the extruded compositions were used to identify potential interactions due to the extrusion processing. IBU exhibited a distinct free acid carbonyl absorption peak at 1709 cm^{-1}, CO–H in-plane bending (hydrogen-bonded) at 1230 cm^{-1}, $–CH_2$ rocking out-of-

Table 2. Printed dose weight accuracy and printed dimensions at various infill densities for the selected inks.

Ink No.	Design	Mean weight (g) ± SD	Length (mm) ± SD	Width (mm) ± SD	Thickness (mm) ± SD
F7	Heart (30% infill)	335.0 ± 5.1	15.0 ± 0.00	15.5 ± 0.05	2.63 ± 0.07
F7	Heart (100% infill)	337.3 ± 5.5	12.7 ± 0.05	12.8 ± 0.08	2.75 ± 0.03
F9	Heart (30% infill)	333.1 ± 4.8	15.0 ± 0.00	15.5 ± 0.05	2.94 ± 0.05
F9	Heart (100% infill)	337.3 ± 5.0	12.3 ± 0.02	12.3 ± 0.05	2.65 ± 0.04

Table 3. IBU content accuracy and individual content uniformity of printed structures.

Ink no.	Theoretical dose (mg)	Measured dose (mg)	Dosed accuracy (± 15%) ± SD	Individual content uniformity (mg)	Measured content uniformity (%)
F7	100	102.0 ± 2.0	2.5 ± 0.6	98.5 ± 0.05	102.0 ± 2.0
F7	100	102.0 ± 2.0	2.4 ± 0.5	102.4 ± 0.08	102.0 ± 2.0
F9	100	102.0 ± 2.0	2.0 ± 0.2	101.5 ± 0.05	102.0 ± 2.0
F9	100	101.0 ± 2.0	2.4 ± 0.2	99.8 ± 0.05	101.0 ± 2.0

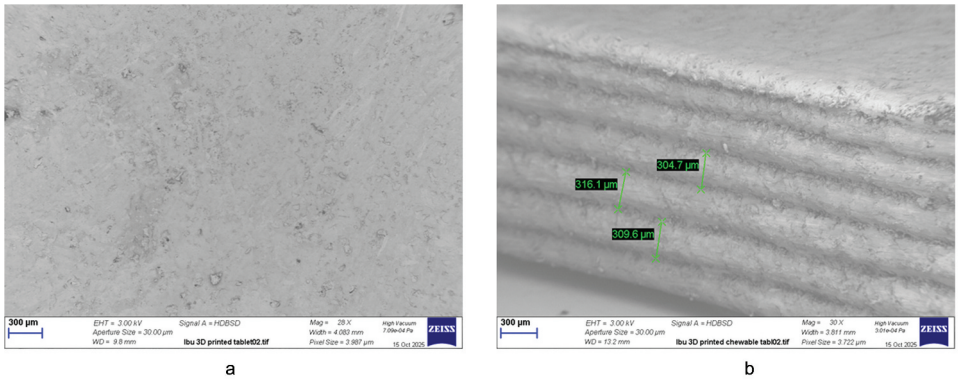

Figure 6. SEM images of the surface morphology of the 3D printed tablet (6a), and 3D printed tablet layer view (6b).

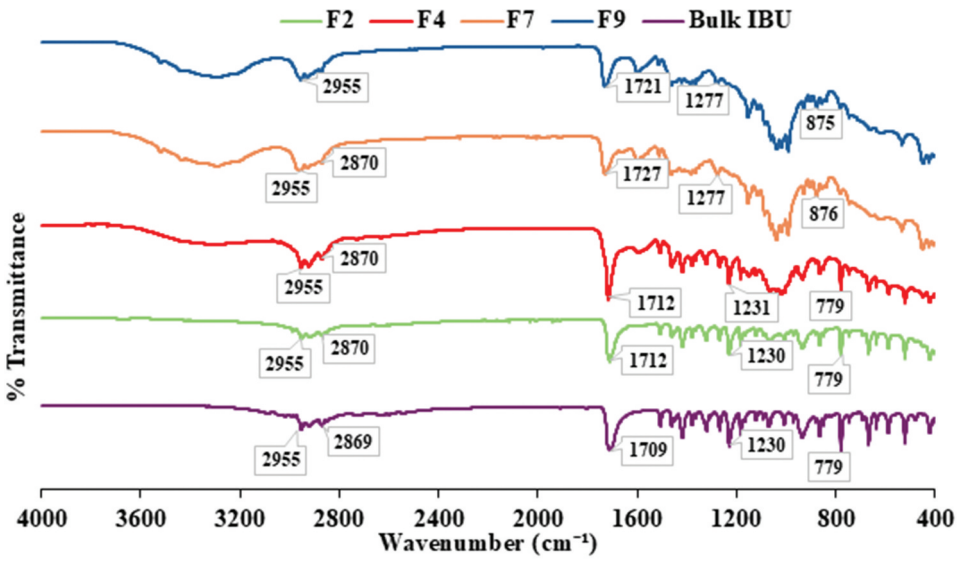

Figure 7. IR Spectra of the bulk IBU, and selected inks including F2. F4, F7 and F9.

plane at 799 cm^{-1}, –C–H out-of-plane deformation at 668 cm^{-1}, and $–CH_2$ in-plane rocking at 522 cm^{-1} [39]. Characteristic absorption bands of EPO were observed at 1146–1240 and 1279 cm^{-1} corresponding to ester functionalities, at 1722 cm^{-1} for the carbonyl group (–C=O), and at 2770–2820 cm^{-1} for the dimethylamine ($R–N^{+}–H$) stretching vibrations [40,41]. In the printed inks, the –C=O stretching band shifted to a wavelength from 1712–1729 cm^{-1} relative to the spectra of the bulk IBU and EPO. Considering the molecular structures of IBU and EPO and recognizing the presence of multiple proton donor and acceptor sites in each EPO monomeric unit, this shift in the –C=O stretching frequency is indicative of hydrogen bond formation between the components. The variation in the wavelengths indicates the degree of interaction between the drug and the polymer.

3.8. Texture analysis and sensory correlation

The textural properties of chewable tablets are intrinsically linked to their sensory performance, which, in conjunction with organoleptic characteristics, plays a pivotal role in patient compliance and acceptability. The texture profile of chewable systems can be delineated into three phases: the initial bite, masticatory, and residual stages, each contributing to the overall sensory perception during consumption.

Selected inks were subjected to a double compression test to evaluate their mechanical behavior (Figure 8), and the corresponding data are summarized in Table 4. Inks F7 and F9, fabricated with a 30% infill density, exhibited significantly lower hardness compared to tablets produced with 100% infill density. The reduction in infill resulted in a marked decrease in hardness (31.6–41.5 N), although cohesiveness remained unaffected, suggesting that matrix integrity was maintained despite structural modification. The printed chewable tablet exhibited relatively high hardness values in comparison to the marketed confectionery gummy bears. Nevertheless, the formulation complies with the August 2018 U.S. FDA guidance on 'Quality Attribute Considerations for Chewable Tablets,' which specifies that chewable tablets should exhibit low hardness values (<12 kp, equivalent to 117.6 N) to ensure chewability [37,42].

Springiness, which reflects the elastic recovery of the material upon deformation, was inversely associated with

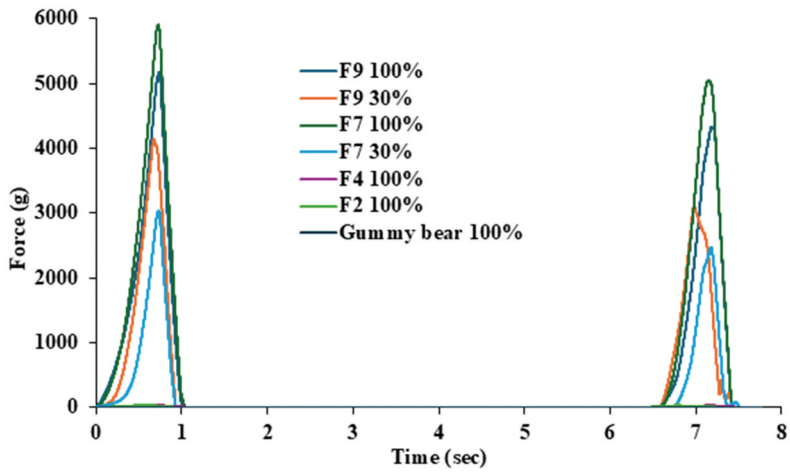

Figure 8. Texture analysis curves of 3D printed IBU chewable tablets and Gummy bear.

Table 4. Textural properties of printed chewable gummies, including cohesiveness, springiness, chewiness, and gumminess.

	Printed structures						
Texture profiles	F2	F4	F7	F7	F9	F9	Gummy bear
Infill density (%)	100.0	100.0	10.00	30.0	100.0	30.0	100.0
Hardness (N)	51.9	43.6	59.8	45.5	54.7	31.6	1.99
Cohesiveness	0.8	0.7	0.8	0.8	0.8	0.8	0.97
Springiness (%)	83.9	65.1	69.0	69.7	68.2	75.5	171.1
Chewiness (N)	34.2	22.6	35.1	25.2	30.1	20.1	3.12
Gumminess (N)	40.7	32.7	50.3	37.4	43.7	26.5	1.92

masticatory effort – lower values correspond to reduced resistance during chewing. All tested inks demonstrated lower springiness compared to commercial gummy bears (Haribo), indicating superior chewability and potentially enhanced patient comfort. In contrast, chewiness quantifies the total energy required to achieve a swallowable consistency during mastication.

The relatively elevated chewiness and gumminess values observed in the 3D-printed chewable tablets are likely attributable to the inclusion of Isomalt sugar (GalenIQ) and cellulose derivatives (CCS), which contribute to viscoelastic network formation within the matrix. Given that mastication involves complex and dynamic mechanical stresses, precise quantification of chewiness remains challenging. Nonetheless, the observed trends highlight the potential of 3D printing to fine-tune the mechanical and sensory characteristics of chewable inks, thereby optimizing patient acceptability and compliance.

3.9. Taste masking evaluation

Effective taste masking of bitter active pharmaceutical ingredients (APIs) is a prerequisite in the development of chewable, gummy-like dosage forms. Pediatric drug formulations are strictly regulated by the European Medicines Agency (2007), and the associated formulation challenges have been extensively documented (Strickley, 2008; 2019) [43].

Consequently, the selection of excipients must be chosen with careful consideration to ensure both efficient taste masking and acceptable palatability. In this study, all excipients were selected based on their approval for use in pediatric inks.

Previous studies have consistently reported the noticeable bitterness of IBU, a finding verified by the current sensory panel, which assigned an average bitterness score of 4 (Figure 9). The strong hydrogen-bonding interactions between IBU and EPO are also known to contribute to effective taste masking [6,44] as reflected in the significantly reduced bitterness score of '1' reported by the panelists. Notably, this evaluation was performed in the presence of other polymers, including the sweetener and the flavoring agents.

Subsequent sensory assessments were conducted on the gummy-like chewable prints to evaluate sweetness intensity and the perception of orange aroma. Previous research has demonstrated that sucralose imparts a strong sweet taste and exhibits synergistic effects with fruit flavors such as orange and strawberry [9,45]. Based on a recent work, the optimal sweetener-to-flavor ratio was determined to be 1.0:1.5, providing enhanced sweetness and aroma perception.

As shown in Table 5, the bulk sucralose was rated as 'very' to 'extremely sweet,' with a pronounced lasting aftertaste, while GalenIQ as 'no sweet.' In contrast, the 3D-printed structures received lower sweetness intensity scores, with most subjects reporting them as 'moderately sweet.' The perceived sweet aftertaste was also notably reduced compared the bulk sucralose. For the orange aroma, the bulk powder exhibited a strong orange and fruity character, whereas the 3D-printed samples were perceived as distinctly 'sweet' and 'fruity,' with a

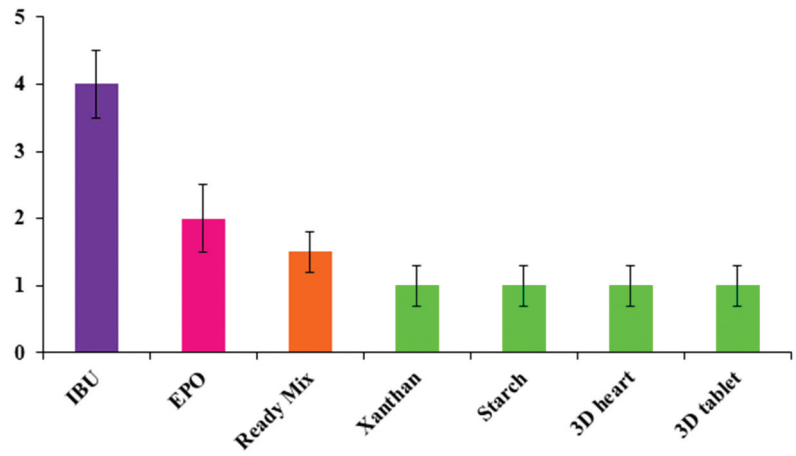

Figure 9. Taste masking evaluation of IBU and the 3D printed gummy-like structures.

Table 5. Panelists ($n = 10$) evaluation on the sweetness and aroma of excipients (powders) and 3D printed gummy-like chewable structures.

	Sweetness				
	No sweet	Moderate sweet	Very sweet	Extremely sweet	Aftertaste
GalenIQ	10	–	—	–	–
Sucralose	–	1–2	8–10	–	8–10
3D tablets	–	8–10	–	–	8–10
	Orange Aroma				
	Sweet	Orange	Sour	Fruity	Aftertaste
Orange	6–8	9–10	–	8–10	5–7
3D tablet	8–10	9–10	–	8–10	8–10

robust aftertaste for both strawberry and orange ink compositions.

These findings highlight the synergistic interactions between sweeteners and flavoring agents, where the combined sensory intensity exceeded that of the individual components. Furthermore, the orange and fruity notes of the 3D-printed tablets remained prominent despite the presence of additional excipients, indicating stability of the flavor perception. Overall, the optimized sweetener-to-flavor ratio yielded excellent taste profiles and demonstrated high efficacy at low concentrations, supporting sucralose's suitability for pediatric chewable dosage forms.

3.10. Effect of composition and infill density on dissolution behavior

Figure 10 presents the *in vitro* drug release profiles of 3D-printed gummy-like structures fabricated with varying infill densities, evaluated alongside the physical mixture and the bulk IBU for comparison. The F9 was selected for optimization, and tablets were printed at four different infill densities of 100%, 70%, 50%, and 30% (Figure 11) to assess the impact of internal structure on dissolution performance. IBU-loaded pellets, approximately 1.5–2 mm in length and 2 mm in diameter, exhibited better dissolution rates in comparison to structures printed with 70% and 100% infill densities. The dissolution rates for the latter were slow, with 45–65% after 30 min.

The most pronounced improvement in dissolution was observed for the printed structures with 30 and 50% infill, densities of 86 and 89%. Overall, printed gummies with a 30–50% infill demonstrated significantly enhanced IBU dissolution with very similar rates compared to those with full (100%) infill.

The crystalline nature of IBU contributed to the low solubility observed in both the bulk drug and physical mixtures at pH 1.2 and 7.2, respectively. During the initial 15 minutes at pH 1.2, only minimal IBU dissolution was detected, consistent with its weakly acidic nature and dissociation constant (pKa = 4.91). Upon adjustment of the medium to pH 7.2, a substantial increase in drug release was observed, reflecting the pH-dependent solubility of IBU.

To further evaluate the influence of formulation composition on IBU release, two distinct IBU inks were employed to fabricate gummy-like heart-shaped designs at 30% and 100% infill densities (Figure 11; ink F9). Two distinct IBU inks were used to print the gummy-like heart-shaped designs, where both inks exhibited visually similar appearances at identical infill densities. Representative photographs of gummies printed at different infill densities using F9 ink are presented in Figure 5.

As anticipated, both inks exhibited faster dissolution rates at 30% infill compared to 100%, confirming the influence of reduced infill density on enhancing drug release.

A comparative analysis of formulations F7 and F9 revealed that F9 achieved superior IBU dissolution rates, regardless of

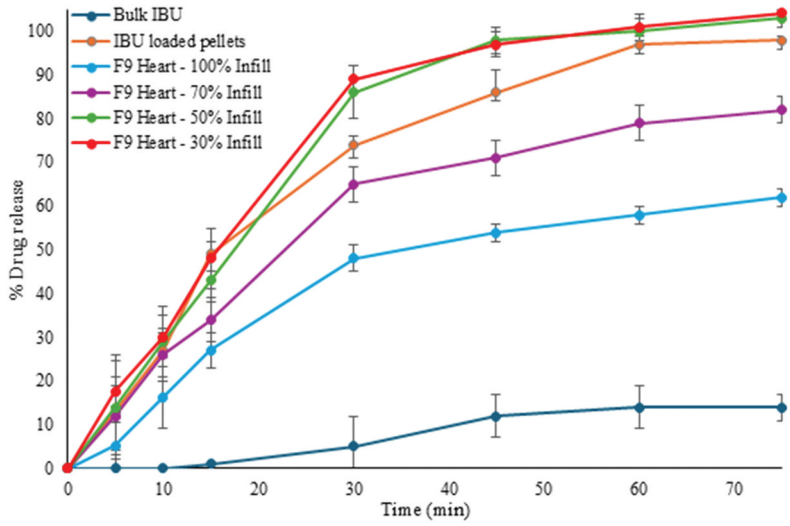

Figure 10. Dissolution profiles of the bulk IBU, PM, IBU-loaded pellets, and gummy-like printed structures with different infills (100%, 70%, 50% and 30%).

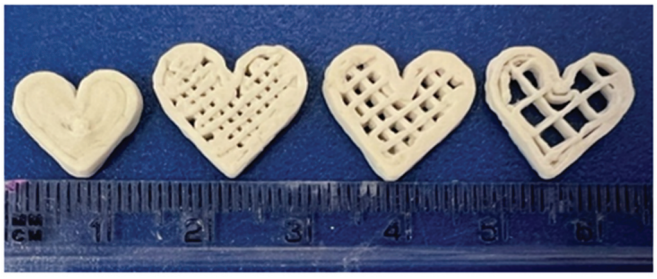

Figure 11. 3D printed tablets (ink F9) with different infills.

infill density. This improvement is attributed to the incorporation of CCS, a highly effective superdisintegrant, in the F9 ink. In contrast, although formulation F7 contained Plasdone-XL, a potent superdisintegrant, the simultaneous inclusion of xanthan gum, functioning as a controlled-release polymer, resulted in notably slower dissolution.

As illustrated in the Figure 12, both the heart-shaped design with 30% infill and the round tablet exhibited the most rapid dissolution, achieving 86–89% drug release within the first 30 minutes. These findings comply with the dissolution requirements outlined in the pharmacopoeia for IBU.

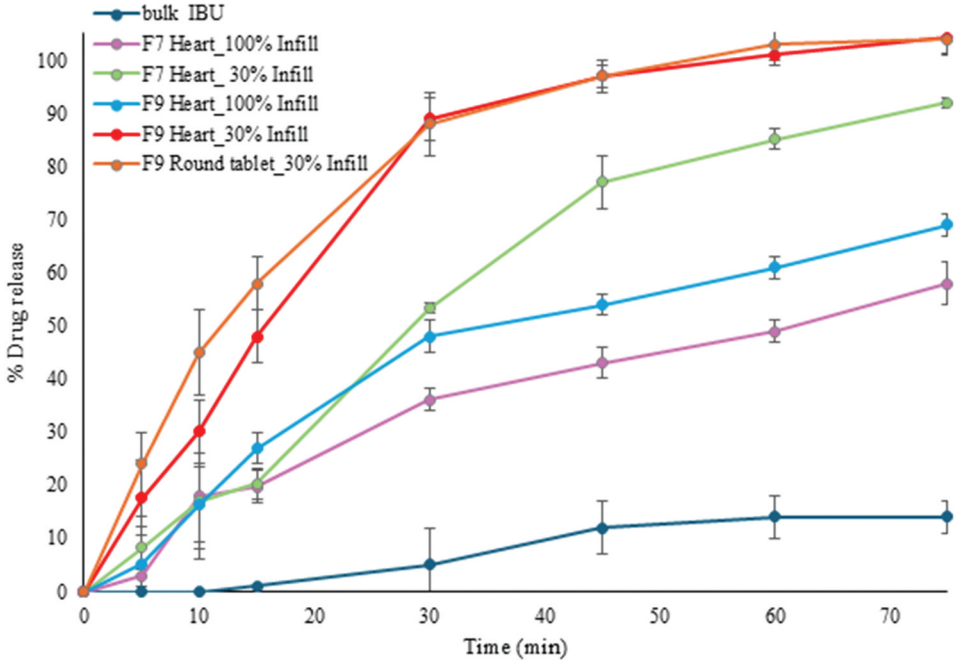

Figure 12. Dissolution profiles of. F7 and F9 compositions at 30 and 100% infill densities of printed gummy-like heart designs.

Overall, the dissolution studies demonstrated that by modulating shape, infill density, and ink composition, it is possible to precisely tailor the drug release profile of 3D-printed, gummy-like formulations [46].

Statistical analysis was performed using Fusion One software, employing a two-way ANOVA *P*-test that revealed a significant difference (Table S1, supplementary) among the *In-vitro* dissolution profiles of the bulk IBU, F9 30%, and F9 100% IBU 3D printed chewable tablets.

Overall, Formulation F9 printed at 30% infill represents the optimal balance among printability, mechanical softness, dissolution performance, and palatability. While other formulations demonstrated acceptable performance in individual tests, F9 (30% infill) consistently achieved superior results across all evaluated quality attributes.

4. Conclusions

This study successfully established a 3D printing platform for the production of chewable, gummy-like pediatric structures containing IBU. Careful optimization of excipient composition, superdisintegrant incorporation, and infill density allowed precise control over extrusion, printability, and structural integrity, where the optimized inks demonstrated superior performance. Rheological characterization confirmed stable shear-thinning behavior, facilitating smooth extrusion and reliable layer adhesion. Drug release profiles were effectively modulated through tablet geometry, infill density, and ink composition, achieving rapid dissolution consistent with pharmacopoeial standards. Taste masking was achieved via hydrogen bonding between IBU and EPO, while optimized sweetener – flavor combinations ensured palatability. Overall, these findings highlight the potential of 3D printing to fabricate pediatric-friendly, chewable dosage forms with controlled mechanical, dissolution, and sensory properties, providing a versatile platform for personalized medicine and improved patient adherence.

Funding

This paper was not funded.

Declarations of interest

The authors have no relevant affiliations or financial involvement with any organization or entity with a financial interest in or financial conflict with the subject matter or materials discussed in the manuscript. This includes employment, consultancies, honoraria, stock ownership or options, expert testimony, grants or patents received or pending, or royalties.

Reviewer disclosures

Peer reviewers on this manuscript have no relevant financial or other relationships to disclose.

Acknowledgments

In compliance with the International Committee of Medical Journal Editors (ICMJE) recommendations, the authors provide the following disclosure regarding the utilization of AI services in this work: During the preparation of this work, the author(s) used ChatGPT 5.1 to improve grammar and spelling. After using this tool/service, the author(s) reviewed and edited the content as needed and take(s) full responsibility for the content of the published article.

Author contributions

Siva S. Kolipaka: Writing – review & editing, Writing – original draft, Software, Investigation, Formal analysis, Validation, Data curation. **Laura A. Junqueira**: Writing – review & editing, Writing – original draft, Formal analysis, Validation, Data curation. **Vivek Garg**: Writing – review & editing, Formal analysis, Validation, Data curation. **Vivek Trivedi**: Writing – review & editing, Writing – original draft, Visualization, Supervision, Resources, Project administration, Funding acquisition. **Dennis Douroumis**: Writing – review & editing, Writing – original draft, Visualization, Supervision, Resources, Project administration, Methodology, Investigation, Data curation, Conceptualization.

Ethical statement

Informed consent was obtained from 10 healthy human subjects, approved by the University of Greenwich's Ethics Committee (protocol code reference number: UG09/10.5.5.12 May 2021).

References

Papers of special note have been highlighted as either of interest (•) or of considerable interest (••) to readers.

1. Quality attribute considerations for chewable tablets guidance for industry | FDA. [cited 2025 May 17]. Available from: https://www.fda.gov/regulatory-information/search-fda-guidance-documents/quality-attribute-considerations-chewable-tablets-guidance-industry
2. Carou-Senra P, Rodríguez-Pombo L, Monteagudo-Vilavedra E, et al. 3D printing of dietary products for the management of inborn errors of intermediary metabolism in pediatric populations. Nutrients. 2023;16(1):61. doi: 10.3390/NU16010061 PMID: 38201891.
3. Douroumis D. Practical approaches of taste masking technologies in oral solid forms. Expert Opin Drug Deliv. 2007;4(4):417–426. doi: 10.1517/17425247.4.4.417 PMID: 17683254.
4. Rodríguez-Pombo L, Awad A, Basit AW, et al. Innovations in chewable formulations: the novelty and applications of 3D printing in drug product design. Pharmaceutics. 2022;14(8):1732. doi: 10.3390/pharmaceutics14081732

•• **A very good article on the development of chewable tablets.**

5. Mennella JA, Spector AC, Reed DR, et al. The bad taste of medicines: overview of basic research on bitter taste. Clin Ther. 2013;35(8):1225. doi: 10.1016/J.CLINTHERA.2013.06.007 PMID: 23886820.
6. Muhindo D, Elkanayati R, Srinivasan P, et al. Recent advances in the applications of additive manufacturing (3D printing) in drug delivery: a comprehensive review. AAPS PharmSciTech. 2023;24(2). doi: 10.1208/S12249-023-02524-9 PMID: 36759435.
7. Dumpa N, Butreddy A, Wang H, et al. 3D printing in personalized drug delivery: an overview of hot-melt extrusion-based fused deposition modeling. Int J Pharm. 2021;600:600. doi: 10.1016/J.IJPHARM.2021.120501 33746011.

•• **A very good article on personalized dosage forms.**

8. Bácskay I, Ujhelyi Z, Fehér P, et al. The evolution of the 3D-Printed drug delivery systems: a review. Pharmaceutics. 2022;14(7):1312. doi: 10.3390/PHARMACEUTICS14071312 35890208.
9. Maniruzzaman M, Boateng JS, Snowden MJ, et al. A review of hot-melt extrusion: process technology to pharmaceutical products. ISRN Pharm. 2012;2012:1–9. doi: 10.5402/2012/436763 23326686.
10. Leister D, Geilen T, Geissler T. Twin-screw extruders for pharmaceutical hot-melt extrusion: technology, techniques and practices. Hot-Melt Extrusion Pharm Appl. 2012:23–42. doi: 10.1002/9780470711415.CH2;SUBPAGE:STRING:ABSTRACT;WEBSITE:WEBSITE:PERICLES;CTYPE:STRING:BOOK
11. Yang Z, Hu Y, Tang G, et al. Development of ibuprofen dry suspensions by hot melt extrusion: characterization, physical stability and

pharmacokinetic studies. J Drug Deliv Sci Technol. 2019;54:101313. doi: 10.1016/J.JDDST.2019.101313
12. Bransford P, Cook J, Gupta M, et al. ICH M9 guideline in development on biopharmaceutics classification system-based biowaivers: an industrial perspective from the IQ consortium. Mol Pharm. 2019;17:361–372. doi: 10.1021/ACS.MOLPHARMACEUT.9B01062
13. Lu M, Guo Z, Li Y, et al. Application of hot melt extrusion for poorly water-soluble drugs: limitations, advances and future prospects. Curr Pharm Des. 2014;20(3):369–387. doi: 10.2174/13816128113199990402 23651401.
14. Bhujbal SV, Mitra B, Jain U, et al. Pharmaceutical amorphous solid dispersion: a review of manufacturing strategies. Acta Pharm Sin B. 2021;11(8):2505–2536. doi: 10.1016/J.APSB.2021.05.014
•• **A very good article of amorphous solid dispersions.**
15. Biedrzycka K, Marcinkowska A. The use of hot melt extrusion to prepare a solid dispersion of ibuprofen in a polymer matrix. Polymers. 2023;15(13):2912. doi: 10.3390/POLYM15132912
16. Mahmood R. Hot melt extrusion: an emerging drug delivery technology. J Dev Drugs. 2017;6(4). doi: 10.4172/2329-6631-C1-022
17. Huang L, Ni W, Jia Y, et al. Process development for the continuous manufacturing of carbamazepine-nicotinamide co-crystals utilizing hot-melt extrusion technology. Pharmaceutics. 2025;17(5):568. doi: 10.3390/pharmaceutics17050568
18. Tambe S, Jain D, Agarwal Y, et al. Hot-melt extrusion: highlighting recent advances in pharmaceutical applications. J Drug Deliv Sci Technol. 2021;63:102452. doi: 10.1016/J.JDDST.2021.102452
19. Simões MF, Pinto RMA, Simões S. Hot-melt extrusion in the pharmaceutical industry: toward filing a new drug application. Drug Discov Today. 2019;24(9):1749–1768. doi: 10.1016/J.DRUDIS.2019.05.013 31132415.
20. Goyanes A, Det-Amornrat U, Wang J, et al. 3D scanning and 3D printing as innovative technologies for fabricating personalized topical drug delivery systems. J Controlled Release. 2016;234:41–48. doi: 10.1016/J.JCONREL.2016.05.034. 27189134.
21. Ullah M, Wahab A, Khan SU, et al. 3D printing technology: a new approach for the fabrication of personalized and customized pharmaceuticals. Eur Polym J. 2023;195:112240. doi: 10.1016/J.EURPOLYMJ.2023.112240
22. Scoutaris N, Ross SA, Douroumis D. 3D printed "starmix" drug loaded dosage forms for paediatric applications. Pharm Res. 2018;35(2). doi: 10.1007/S11095-017-2284-2 29368113.
•• **A very good article on the development of paediatric dosage forms.**
23. Tegegne AM, Ayenew KD, Selam MN. Review on recent advance of 3DP-based pediatric drug formulations. Biomed Res Int. 2024;2024(1):4875984. doi: 10.1155/2024/4875984 39364267.
24. Karavasili C, Gkaragkounis A, Moschakis T, et al. Pediatric-friendly chocolate-based dosage forms for the oral administration of both hydrophilic and lipophilic drugs fabricated with extrusion-based 3D printing. Eur J Pharmaceut Sci. 2020;147:105291. doi: 10.1016/J.EJPS.2020.105291 32135271.
25. Liu Z, Huang J, Fang D, et al. Material extrusion 3D-printing technology: a new strategy for constructing water-soluble, high-dose, sustained-release drug formulations. Mater Today Bio. 2024;27:101153. doi: 10.1016/J.MTBIO.2024.101153
26. Tabriz AG, Hui HW, Boersen N, et al. 3D printed flavor-rich chewable pediatric tablets fabricated using microextrusion for point of care applications. Mol Pharm. 2023;20(6):2919–2926. doi: 10.1021/ACS.MOLPHARMACEUT.2C01061 37022302.
• **A very good article of 3D printed chewable tablets.**
27. Tabriz AG, Scoutaris N, Gong Y, et al. Investigation on hot melt extrusion and prediction on 3D printability of pharmaceutical grade polymers. Int J Pharm. 2021;604:120755. doi: 10.1016/J.IJPHARM.2021.120755 34052338.
28. Debnath SK, Debnath M, Srivastava R, et al. Intervention of 3D printing in health care: transformation for sustainable development. Expert Opin Drug Deliv. 2021;18(11):1659–1672. doi: 10.1080/17425247.2021.1981287 34520310.
29. Huanbutta K, Burapapadh K, Sriamornsak P, et al. Practical application of 3D printing for pharmaceuticals in hospitals and pharmacies. Pharmaceutics. 2023;15(7):1877. doi: 10.3390/PHARMACEUTICS15071877 37514063.
30. Wang S, Chen X, Han X, et al. A review of 3D printing technology in Pharmaceutics: technology and applications, now and future. Pharmaceutics. 2023;15(2):416. doi: 10.3390/PHARMACEUTICS15020416 36839738.
31. Lima AL, Gross IP, de Sá-Barreto LL, et al. Extrusion-based systems for topical and transdermal drug delivery. Expert Opin Drug Deliv. 2023;20(7):979–992. doi: 10.1080/17425247.2023.2241362
32. Shah VP, Lesko LJ, Fan J, et al. FDA guidance for industry 1 dissolution testing of immediate release solid oral dosage forms. Dissolut Technol. 1997;4(4):15–22. doi: 10.14227/DT040497P15 37522812.
33. Dissolution Methods. [cited 2026 Jan 19]. Available from: https://www.accessdata.fda.gov/scripts/cder/dissolution/dsp_SearchResults.cfm
34. Anand O, Yu LX, Conner DP, et al. Dissolution testing for generic drugs: an FDA perspective. AAPS J. 2011;13(3):328. doi: 10.1208/S12248-011-9272-Y 21479700.
35. Mundhe R, Folane P, Biyani KR. Review on efficacy of chewable tablets in improving oral drug delivery. Int J Pharm Sci. 2025;3:696. doi: 10.5281/ZENODO.14997565
36. Subbaraman B, Peek N. p5.fab: direct control of digital fabrication machines from a creative coding environment. In: Mueller FF, Greuter S, editors. DIS 2022 - Proceedings of the 2022 ACM Designing Interactive Systems Conference: Digital Wellbeing; Australia. New York, USA: Association for Computing Machinery; 2022 June 13–17. p. 1148–1161. doi: 10.1145/3532106.3533496
37. Somireddy M, Czekanski A, Czekanski A, et al. mechanical characterization of additively manufactured parts by FE modeling of mesostructure. J Manuf Mater Process. 2017;1(2):1. doi: 10.3390/JMMP1020018
38. Gonabadi H, Chen Y, Yadav A, et al. Investigation of the effect of raster angle, build orientation, and infill density on the elastic response of 3D printed parts using finite element microstructural modeling and homogenization techniques. Int J Adv Manuf Technol. 2021;118(5):1485–1510. doi: 10.1007/S00170-021-07940-4
39. Acharya M, Mishra S, Sahoo RN, et al. Infrared spectroscopy for analysis of co-processed ibuprofen and magnesium trisilicate at milling and freeze drying. Acta Chim Slov. 2017;64:45–54. doi: 10.17344/ACSI.2016.2772 28380218.
40. Linares V, Yarce CJ, Echeverri JD, et al. Relationship between degree of polymeric ionisation and hydrolytic degradation of Eudragit® E polymers under extreme acid conditions. Polymers (Basel). 2019;11(6):11. doi: 10.3390/POLYM11061010 31181597.
41. De Brabander C, Van Den Mooter G, Vervaet C, et al. Characterization of ibuprofen as a nontraditional plasticizer of ethyl cellulose. J Pharm Sci. 2002;91(7):1678–1685. doi: 10.1002/jps.10159 12115829.
42. Quality attribute considerations for chewable tablets guidance for industry. [cited 2026 Jan 20]. Available from: https://www.fda.gov/files/drugs/published/Quality-Attribute-Considerations-for-Chewable-Tablets-Guidance-for-Industry.pdf
43. Maniruzzaman M, Boateng JS, Chowdhry BZ, et al. A review on the taste masking of bitter APIs: hot-melt extrusion (HME) evaluation. Drug Dev Ind Pharm. 2014;40(2):145–156. doi: 10.3109/03639045.2013.804833 23763436.
44. Bandari S, Nyavanandi D, Dumpa N, et al. Coupling hot melt extrusion and fused deposition modeling: critical properties for successful performance. Adv Drug Deliv Rev. 2021;172:52–63. doi: 10.1016/J.ADDR.2021.02.006 33571550.
•• **A very good article on coupling processing technologies.**
45. Cherian S, Lee BS, Tucker RM, et al. Toward improving medication adherence: the suppression of bitter taste in edible taste films. Adv Pharmacol Sci. 2018;2018:1–11. doi: 10.1155/2018/8043837 30046304.
46. McDonagh T, Belton P, Qi S. Manipulating drug release from 3D printed dual-drug loaded polypills using challenging polymer compositions. Int J Pharm. 2023;637:122895. doi: 10.1016/J.IJPHARM.2023.122895 36972779.